

Supplementary Materials for

Enhanced economic connectivity to foster heat stress–related losses

Leonie Wenz and Anders Levermann

Published 10 June 2016, *Sci. Adv.* **2**, e1501026 (2016)

DOI: 10.1126/sciadv.1501026

The PDF file includes:

- Description of the model acclimate
- fig. S1. Examples of forcing time series of first-order daily production loss due to heat stress.
- fig. S2. Independence of main result on modeling assumptions.
- fig. S3. Annually averaged global mean temperature over time.
- fig. S4. Contribution of first-order and higher-order losses to total annual production loss.
- fig. S5. Mean value from log-log histogram of regional SPC values.
- fig. S6. Heat stress–induced production losses under the RCP 8.5 warming scenario for different economic structures over time.
- table S1. Alphabetical list of all sectors used in simulations.
- table S2. Alphabetical list of all countries used in simulations.

Supplementary Materials

Description of the model *acclimate*

The numerical model *acclimate* (51, 52) describes the propagation of climate-induced production losses along global supply chains. It builds on a network representation of intra- and interregional economic relationships. The nodes in this network are production and consumption sites that are linked by input and output flows (in USD per day) derived from annual multi-regional input-output matrices (49). The total number of production and consumption sites is hence given by the data (in this study: 186 regions and 27 industry sectors including final demand, i.e. about 5000 sites). To explain the main mechanisms of the model, we here focus on an exemplary production site represented by the index pair js where j denotes the good being produced and s the region the site is located in. It is connected to other production sites ir and ku via input ($Z_{ir \rightarrow js}^*$) and output flows ($Z_{js \rightarrow ku}^*$).

The economic state given by the data serves as a baseline for the model (marked by the index $*$) whose evolution over time is not explicitly modeled. Instead the model simulates the response to small perturbations (here: daily production losses due to heat-stress) after which it strives back to this initial state. It operates on discrete time steps of length $\Delta t = 1$ day thereby introducing dynamics on the input-output flows.

The model accounts for geographically-motivated transit times $\tau_{ir \rightarrow js}$ that are required to transport a good i from a region r to a production site js . The transport stock, i.e. total amount of good i from region r that is being transported to production site js at time step $(t + 1)$, is given by

$$T_{ir \rightarrow js}^{(t+1)} = \sum_{b=0}^{\tau_{ir \rightarrow js} - 1} Z_{ir \rightarrow js}^{(t+1-b)} \cdot \Delta t$$

All goods i arriving at production site js at time step $(t + 1)$ add up to the total input flow $I_{i \rightarrow js}^{(t+1)}$ that is stored in an input-storage. The initial content $S_{i \rightarrow js}^* = \psi_i \cdot I_{i \rightarrow js}^*$ of this input-storage is a multiple of the initial input flow $I_{i \rightarrow js}^*$, where the parameter ψ_i expresses for how many days a production site can keep its production up if input i is lacking. The storage content $S_{i \rightarrow js}^{(t+1)}$ at time $(t + 1)$ can exceed this initial content at most by a factor ω_i . It equals $S_{i \rightarrow js}^{(t)}$ unless the amount $U_{i \rightarrow js}^{(t)}$ of good i that was taken from the storage for production in the last time step differs from the number of inputs at that time:

$$S_{i \rightarrow js}^{(t+1)} = \max \left(\min \left(\omega_i \cdot S_{i \rightarrow js}^*, \quad S_{i \rightarrow js}^{(t)} + \Delta t \left(I_{i \rightarrow js}^{(t)} - U_{i \rightarrow js}^{(t)} \right) \right), \quad 0 \right)$$

Without an external perturbation, production site js uses its current inputs for production. In case the amount of inputs is not sufficient, it reverts to its input-storages. The possible use flow $\hat{U}_{i \rightarrow js}^{(t+1)}$ of good i at time $(t + 1)$ is hence given by

$$\hat{U}_{i \rightarrow js}^{(t+1)} = I_{i \rightarrow js}^{(t+1)} + \frac{S_{i \rightarrow js}^{(t+1)}}{\Delta t}$$

The maximum amount of output js can produce at time $(t + 1)$ is determined by the inputs that are available then, i.e. $\hat{U}_{i \rightarrow js}^{(t+1)}$ of all intermediate input goods i . The model thereby relies on the assumption of perfect complementarity which means that the minimum of the relative availability of one input good across all input goods determines the maximum relative productivity. The possible production ratio $\hat{p}_{js}^{(t+1)}$ of js at time $(t + 1)$ that may also be limited to $\lambda_{js}^{(t+1)} \in [0,1]$ through an external perturbation reads

$$\hat{p}_{js}^{(t+1)} = \min \left(\min_i \left(\frac{\hat{U}_{i \rightarrow js}^{(t+1)}}{U_{i \rightarrow js}^*} \right), \lambda_{js}^{(t+1)} \right)$$

The actual production of js is determined not only by the availability of its intermediate inputs and a potential external forcing (possible production ratio $\hat{p}_{js}^{(t+1)}$) but also by the demand requests it has received in the last time step (target production ratio $\tilde{p}_{ku}^{(t+1)}$).

The demand $D_{j \leftarrow ku}^{(t)}$ of any other production site, ku , for product j at time (t) is determined as follows: As long as the input-storage content (including all goods j that are being transported to ku at that time) remains constant, $D_{j \leftarrow ku}^{(t)}$ equals the target use flow $\tilde{U}_{j \rightarrow ku}^{(t)}$ of product j at that time. This flow $\tilde{U}_{j \rightarrow ku}^{(t)}$ reflects the amount of good j that was or would have been necessary in order to fulfill all demand requests in that time step considering the imposed forcing $\lambda_{ku}^{(t)}$. Otherwise, the demand is set such as to balance the difference. If the storage has decreased, the demand is increased in order to refill the storage within a certain time-frame regulated by the parameter γ_j . If by contrast the storage content has increased because the production site ku has not used all its inputs j , the demand decreases. Accordingly, $D_{j \leftarrow ku}^{(t)}$ is given by

$$D_{j \leftarrow ku}^{(t)} = \max \left(\tilde{U}_{j \rightarrow ku}^{(t)} + \frac{(S_{j \rightarrow ku}^* + \sum_s T_{js \rightarrow ku}^* - S_{j \rightarrow ku}^{(t)} - \sum_s T_{js \rightarrow ku}^{(t)})}{\gamma_j}, 0 \right)$$

with $\tilde{U}_{j \rightarrow ku}^{(t)} = \tilde{p}_{ku}^{(t)} \cdot \lambda_{ku}^{(t)} \cdot U_{j \rightarrow ku}^*$.

Once a production site ku has determined its demand for good j , it distributes it among its respective suppliers considering how reliable each supplier has been, in diminishing shares weighted by the parameter $\varphi \in]0,1]$, in the last time steps. Production site js thus receives the following demand request from ku at time (t) :

$$D_{js \leftarrow ku}^{(t)} = \frac{\theta_{js \rightarrow ku}^{(t)} \cdot Z_{js \rightarrow ku}^*}{\sum_{s'} \theta_{js' \rightarrow ku}^{(t)} \cdot Z_{js' \rightarrow ku}^*} \cdot D_{j \leftarrow ku}^{(t)}$$

with

$$\theta_{js \rightarrow ku}^{(t)} = \varphi \cdot \theta_{js \rightarrow ku}^{(t-1)} + (1 - \varphi) \cdot \vartheta_{js \rightarrow ku}^{(t)}$$

and

$$\vartheta_{js \rightarrow ku}^{(t)} = \frac{Z_{js \rightarrow ku}^{(t)}}{D_{js \leftarrow ku}^{(t-1)}}$$

The sum of all demand requests $D_{js \leftarrow ku}^{(t)}$ that js receives from different purchasers ku at time (t) determines its target production ratio $\tilde{p}_{js}^{(t+1)}$ in the next time step:

$$\tilde{p}_{js}^{(t+1)} = \frac{\sum_k \sum_u D_{js \leftarrow ku}^{(t)}}{X_{js}^*}$$

where $X_{js}^* = \sum_k \sum_u Z_{js \rightarrow ku}^* = \sum_k \sum_u D_{js \leftarrow ku}^*$ denotes its initial production. The production ratio then reads

$$p_{js}^{(t+1)} = \min \left(\tilde{p}_{js}^{(t+1)}, \hat{p}_{js}^{(t+1)} \right)$$

and the total production is given by

$$X_{js}^{(t+1)} = p_{js}^{(t+1)} \cdot X_{js}^*$$

This output is then distributed equally among all purchasers:

$$Z_{js \rightarrow ku}^{(t+1)} = \frac{D_{js \leftarrow ku}^{(t)}}{\sum_{k'} \sum_{u'} D_{js \leftarrow k'u'}^{(t)}} \cdot X_{js}^{(t+1)}$$

A consumption site $j_f s$ is a slightly modified production site. Analogously, it has input storages and addresses demand requests. Unlike production, consumption is however not limited by the

assumption of perfect complementarity. Therefore, the total amount of good i that a consumption site j_{fs} consumes at time $(t + 1)$ is given by

$$C_{i \rightarrow j_{fs}}^{(t+1)} = U_{i \rightarrow j_{fs}}^{(t+1)} = c_{i \rightarrow j_{fs}}^{(t+1)} \cdot U_{i \rightarrow j_{fs}}^*$$

where the consumption ratio $c_{i \rightarrow j_{fs}}^{(t+1)}$ reads

$$c_{i \rightarrow j_{fs}}^{(t+1)} = \min \left(\frac{\hat{U}_{i \rightarrow j_{fs}}^{(t+1)}}{U_{i \rightarrow j_{fs}}^*}, \lambda_{i \rightarrow j_{fs}}^{(t+1)} \right)$$

Figures and Tables

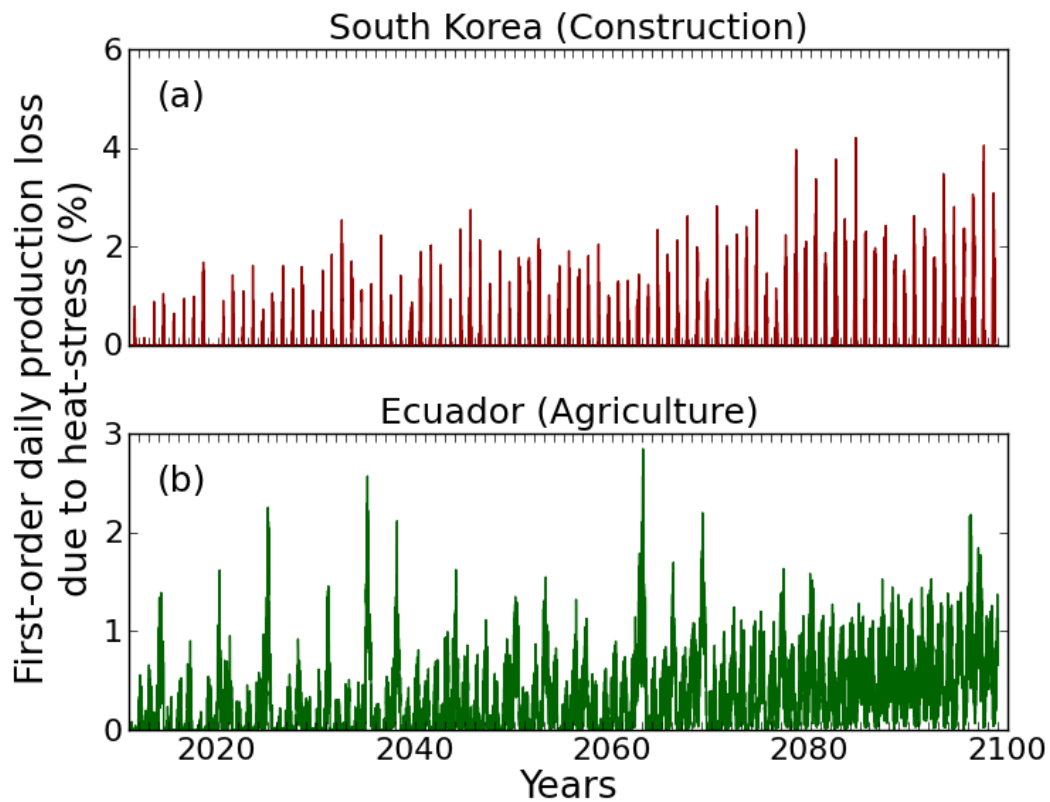


fig. S1. Examples of forcing time series of first-order daily production loss due to heat stress. Following econometric observations, daily economic output of the South Korean construction **(Panel a)** and the Ecuadorian agriculture **(Panel b)** sectors is reduced by 0.8 and 0.6%, respectively, for each additional degree above 27°C. This imposes a shock-like forcing upon the production of these regional sectors (exemplified here for the economic base year 2011). For most of the study only observed temperatures between the years 1991 and 2011 were used. Here we show the projections under the climate-change scenario RCP-8.5 in order to illustrate the future trend in the forcing.

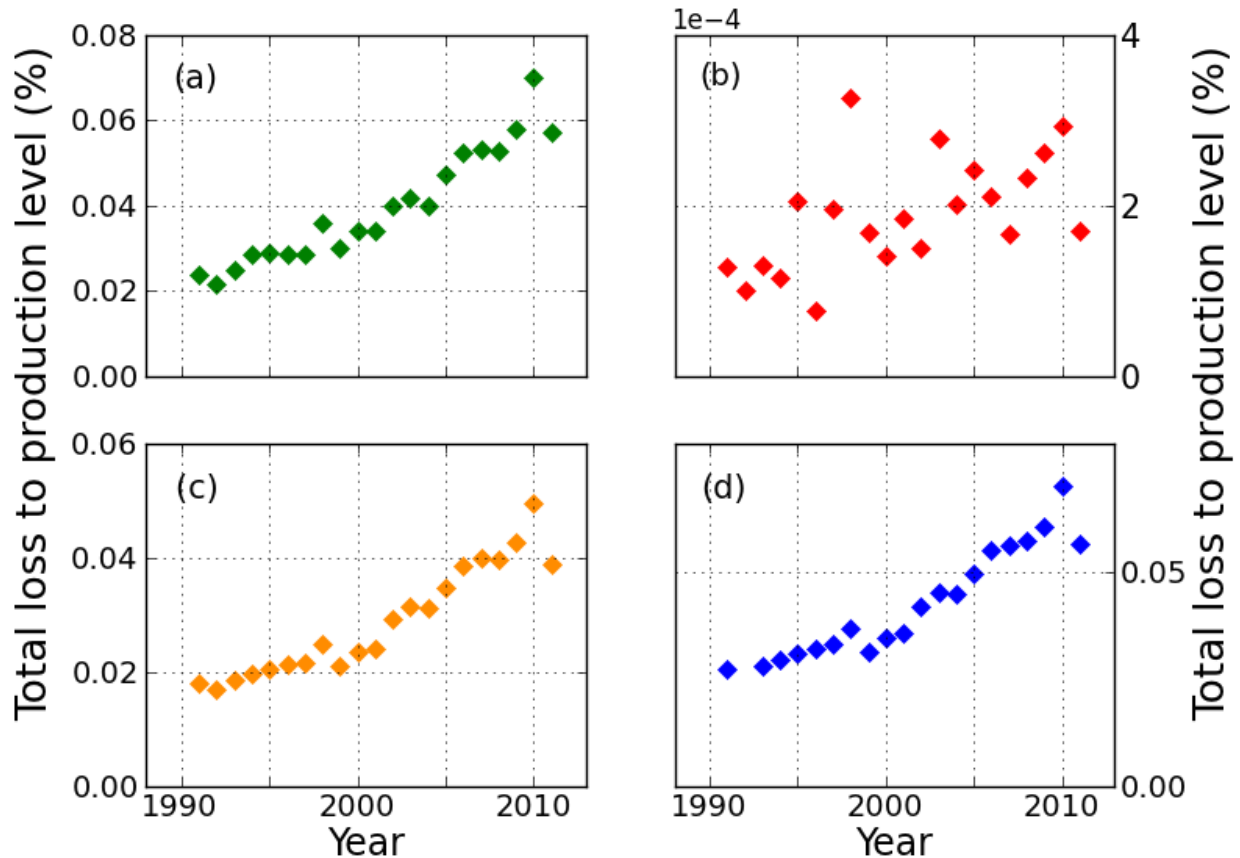


fig. S2. Independence of main result on modeling assumptions. Relative production losses under different scenarios increase over time. **Panel a: Heat-stress in all countries.** The relationship of temperature to labor productivity is not only applied to tropical countries but to all countries (186 in total). **Panel b: Heat-stress in the Caribbean and Central America.** The relationship of temperature to labor productivity is applied to countries in the Caribbean and Central America only (19 in total). **Panel c: Heat-stress in the tropics with fixed cut-off threshold for economic flows.** Very small flows from the annual input-output data are not filtered according to a variable threshold relative to the total flow volume in that year but according to a fixed threshold of 1 M USD (per year). **Panel d: Heat-stress in the tropics for temperature above 26°C.** It is assumed that the relationship of temperature to labor productivity already holds for temperature above 26°C instead of 27°C.

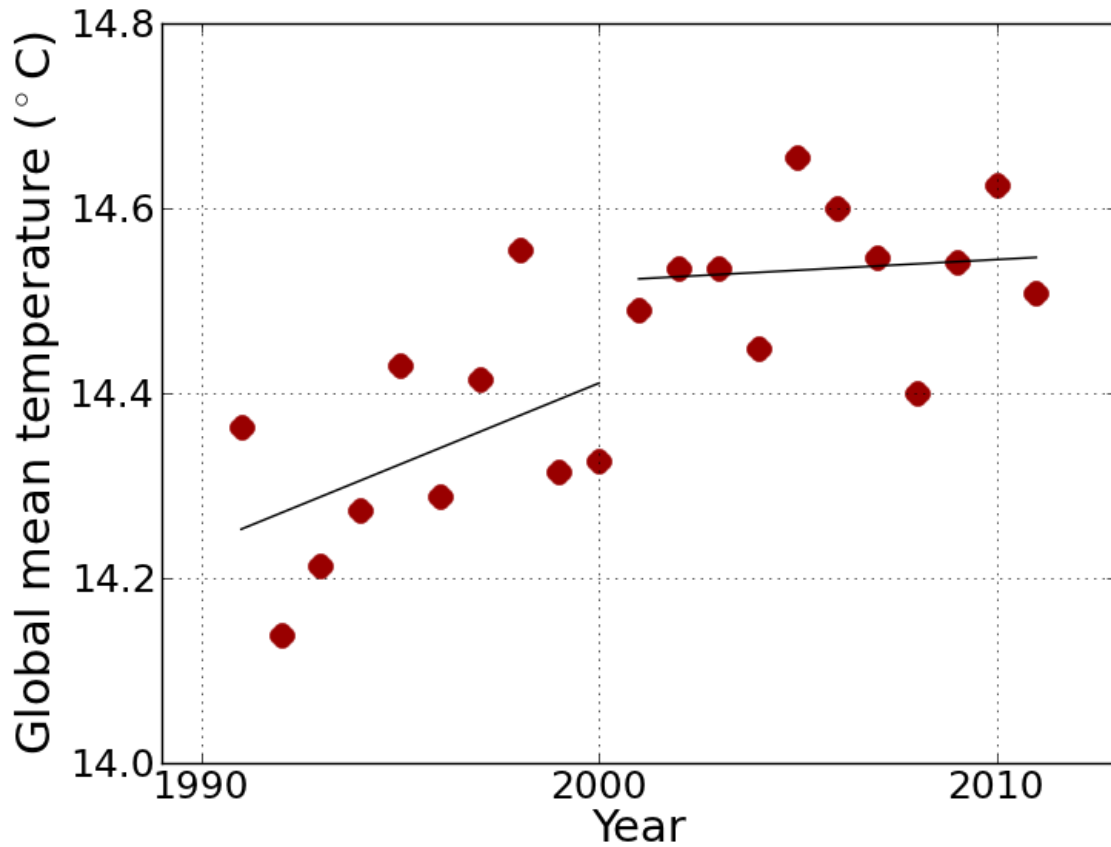


fig. S3. Annually averaged global mean temperature over time. Observation-based time series of annually averaged global mean temperature shows a trend in the 1991-2000-period but no trend in in the 2001-2011-period. Here, the time series of the WFDEI meteorological forcing data set (57) where the WATCH forcing data methodology was applied to ERA-interim reanalysis data (58) were used.

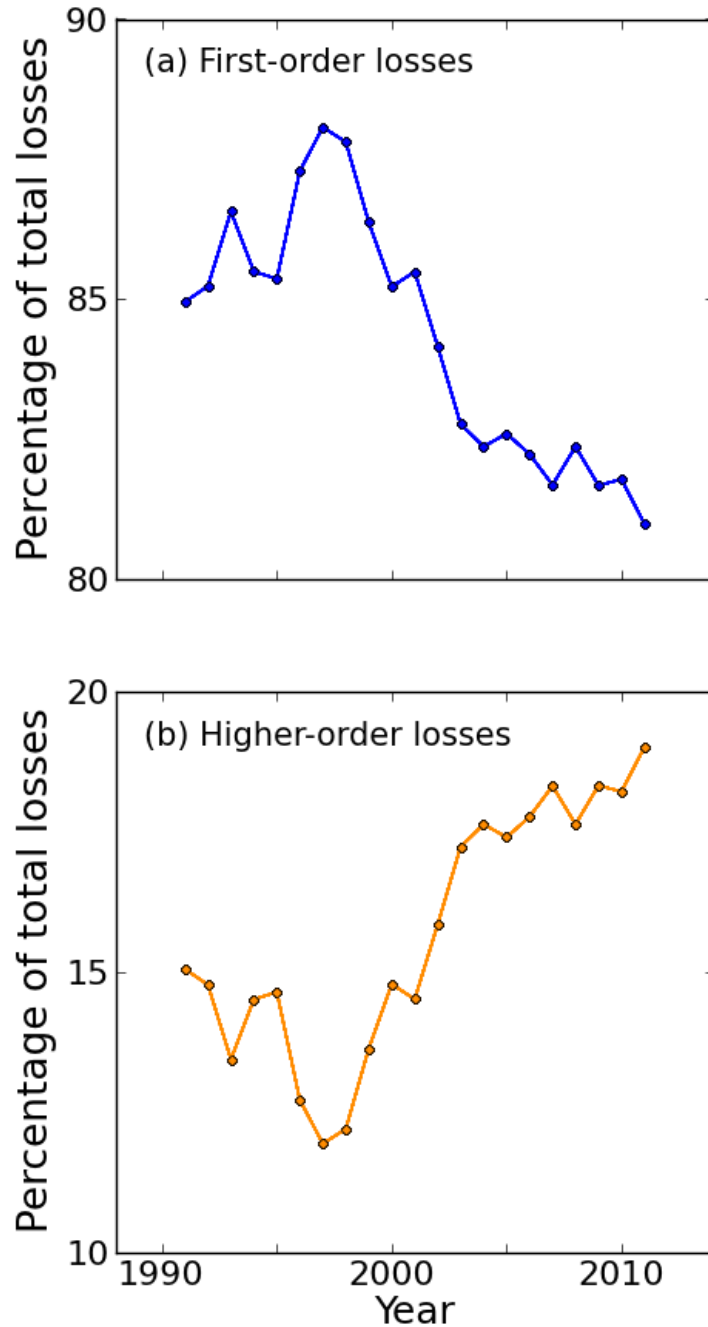


fig. S4. Contribution of first-order and higher-order losses to total annual production loss.

First-order losses denote heat-stress-induced reductions in output of regional sectors (where the initial production level is given by multi-regional input-output data; compare Fig. 1). They can induce further productions reductions (*higher-order losses*) through linkages in the global supply network. The sum of all first- and higher-order losses per year yields the total loss in that year. While the share of first-order production losses as a percentage of total losses declines from 2001 on (Panel a), that of higher-order production losses increases (Panel b).

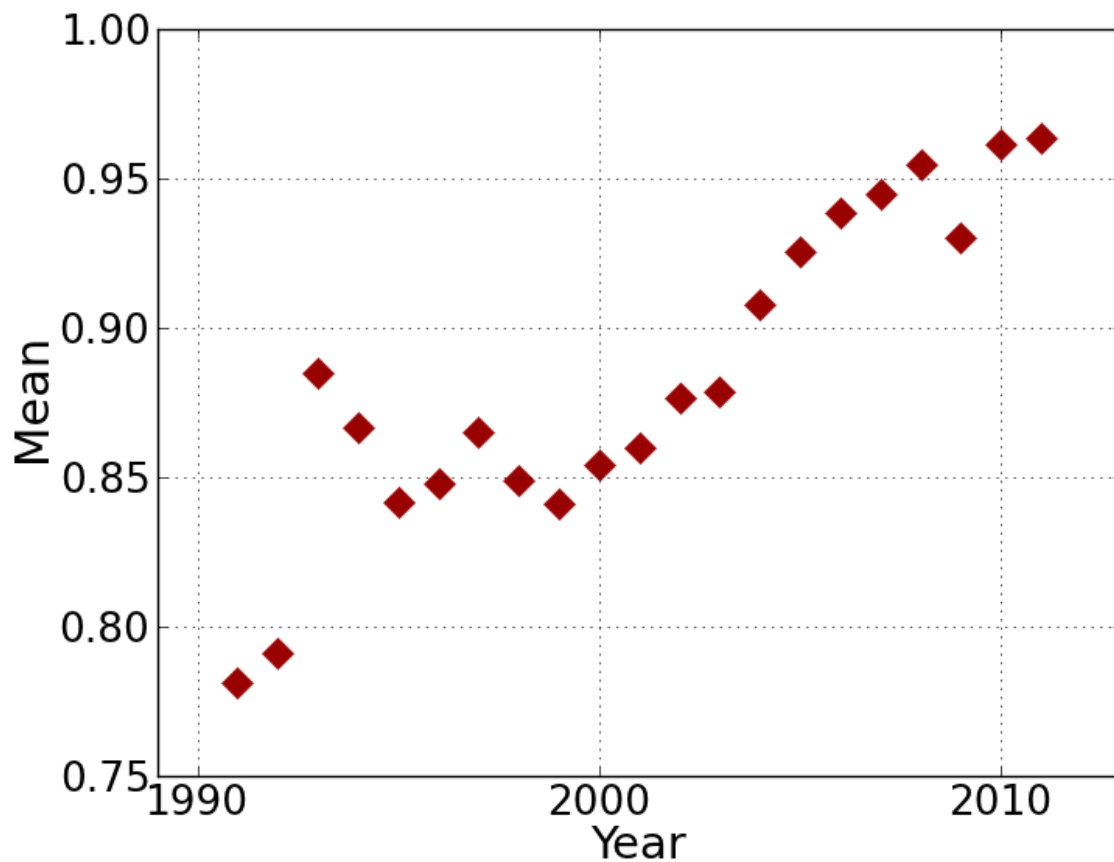


fig. S5. Mean value from log-log histogram of regional SPC values. Mean value of log-log frequency distribution of regional SPC values (Fig. 6B) increases over time. While the trend is not as clear in the 1990s, it becomes evident from 2001 on indicating that the distribution has been shifted towards higher values over time.

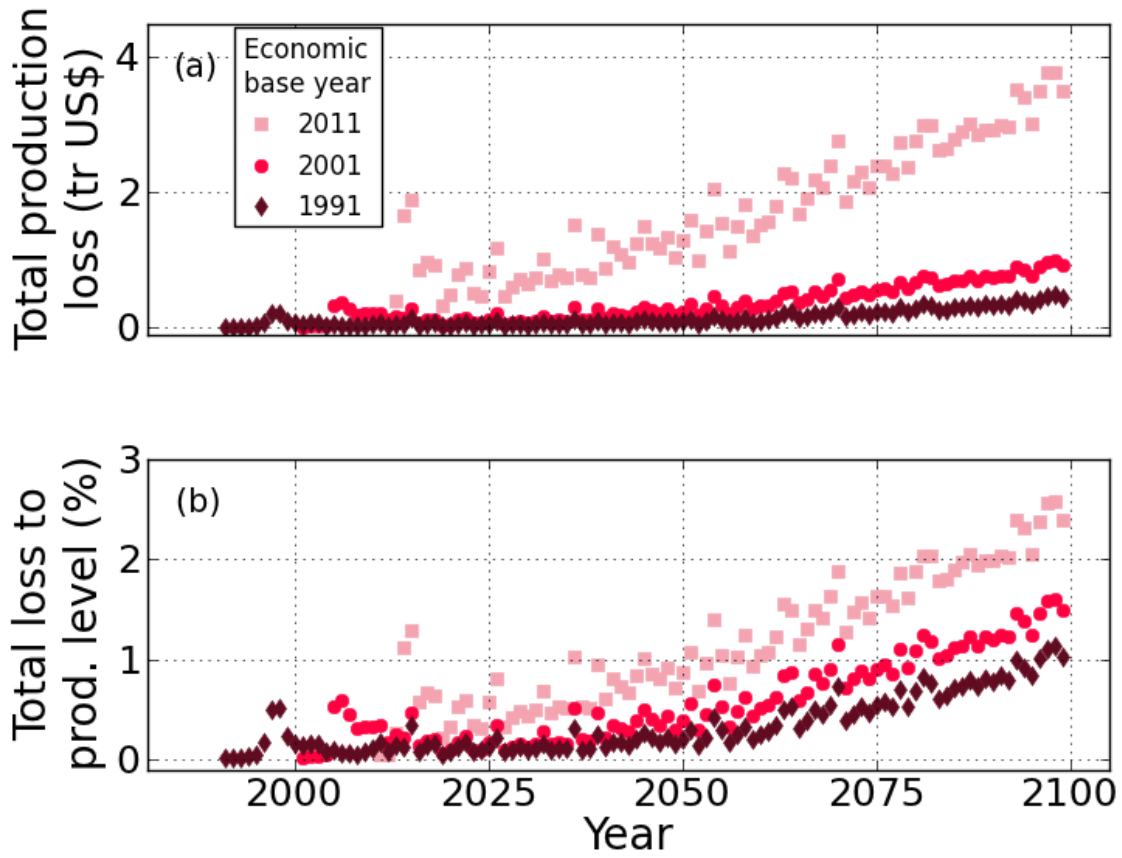


fig. S6. Heat-stress-induced production losses under the RCP 8.5 warming scenario for different economic structures over time. Panel a: Total production losses. Total production losses increase over time for different economic base years (here: 1991, 2001 and 2011) of the economic structure. **Panel b: Relative production losses.** Annual production losses as a share of total annual production increase over time for different economic base years.

table S1. Alphabetical list of all sectors used in simulations. Grey background denotes that the sector is assumed to be subjected to heat-stress in tropical countries. The percentage by which the output is reduced for each additional degree above 27°C is given in brackets.

Agriculture (0.8%)	Transport Equipment	Transport
Fishing (0.8%)	Other Manufacturing	Post and Telecommunications
Mining and Quarrying (4.2%)	Recycling	Financial Intermediation and Business Activities
Food & Beverages	Electricity, Gas and Water	Public Administration
Textiles and Wearing Apparel	Construction (0.6%)	Education, Health and Other Services
Wood and Paper	Maintenance and Repair	Private Households
Petroleum, Chemical and Non-Metallic Mineral Products	Wholesale Trade	Others
Metal Products	Retail Trade	Re-export & Re-import
Electrical and Machinery	Hotels and Restaurants	Final Demand

table S2. Alphabetical list of all countries used in simulations. Grey background denotes that countries are predominantly located in a belt between 30°N and 30°S around the equator. Very small tropical countries, as e.g. Aruba, were not captured by the temperature mask. Given their comparably minor contribution to the overall production level, they are not considered when computing the effects of heat-stress.

Afghanistan	Cambodia	French Polynesia	Latvia	Niger	South Africa
Albania	Cameroon	Gabon	Lebanon	Nigeria	Spain
Algeria	Canada	Gambia	Lesotho	Norway	Sri Lanka
Andorra	Cap Verde	Georgia	Liberia	Palestine	Suriname
Angola	Cayman Islands	Germany	Libya	Oman	Swaziland
Antigua and Barbuda	Central African Republic	Ghana	Liechtenstein	Pakistan	Sweden
Argentina	Chad	Greece	Lithuania	Panama	Switzerland
Armenia	Chile	Greenland	Luxembourg	Papua New Guinea	Syria
Aruba	China	Guatemala	Macao	Paraguay	Taiwan
Australia	Colombia	Guinea	Madagascar	Peru	Tajikistan
Austria	PR Congo	Guyana	Malawi	Philippines	Thailand
Azerbaijan	Costa Rica	Haiti	Malaysia	Poland	Macedonia
Bahamas	Croatia	Honduras	Maldives	Portugal	Togo
Bahrain	Cuba	Hong Kong	Mali	Qatar	Trinidad and Tobago
Bangladesh	Cyprus	Hungary	Malta	South Korea	Tunisia
Barbados	Czech Republic	Iceland	Mauritania	Moldova	Turkey
Belarus	Côte d'Ivoire	India	Mauritius	Romania	Turkmenistan
Belgium	North Corea	Indonesia	Mexico	Russia	Uganda
Belize	DR Congo	Iran	Monaco	Rwanda	Ukraine
Benin	Denmark	Iraq	Mongolia	Samoa	United Arab Emirates
Bermuda	Djibouti	Ireland	Montenegro	San Marino	United Kingdom
Bhutan	Dominican Republic	Israel	Morocco	Sao Tomé and Príncipe	Tanzania
Bolivia	Ecuador	Italy	Mozambique	Saudi Arabia	United States of America
Bosnia and Herzegovina	Egypt	Jamaica	Myanmar	Senegal	Uruguay
Botswana	El Salvador	Japan	Namibia	Serbia	Uzbekistan
Brazil	Eritrea	Jordan	Nepal	Seychelles	Vanuatu
British Virgin Islands	Estonia	Kazakhstan	Netherlands	Sierra Leone	Venezuela
Brunei	Ethiopia	Kenya	Netherlands Antilles	Singapore	Vietnam
Bulgaria	Fiji	Kuwait	New Caledonia	Slovakia	Yemen
Burkina Faso	Finland	Kyrgyzstan	New Zealand	Slovenia	Zambia
Burundi	France	Laos	Nicaragua	Somalia	Zimbabwe